Cellular Signalling 58 (2019) 53–64

Contents lists available at ScienceDirect

Cellular Signalling

journal homepage: www.elsevier.com/locate/cellsig

Lactate accelerates calcification in VSMCs through suppression of BNIP3-mediated mitophagy

Yi Zhu[a], Jing-Jing Ji[a], Rui Yang[b], Xi-Qiong Han[a], Xue-Jiao Sun[a], Wen-Qi Ma[a], Nai-Feng Liu[a,*]

[a] Department of Cardiology, Zhongda Hospital, School of Medicine, Southeast University, Nanjing 210009, PR China
[b] Pharmaceutical Department, Shandong Provincial Qianfoshan Hospital, Jinan 250014, PR China

ARTICLE INFO

Keywords:
Lactate
VSMC
Vascular calcification
Autophagy
Mitophagy

ABSTRACT

Arterial media calcification is one of the major complications of diabetes mellitus, which is related to oxidative stress and apoptosis. Mitophagy is a special regulation of mitochondrial homeostasis and takes control of intracellular ROS generation and apoptotic pathways. High circulating levels of lactate usually accompanies diabetes. The potential link between lactate, mitophagy and vascular calcification is investigated in this study. Lactate treatment accelerated VSMC calcification, evaluated by measuring the calcium content, ALP activity, RUNX2, BMP-2 protein levels, and Alizarin red S staining. Lactate exposure caused excessive intracellular ROS generation and VSMC apoptosis. Lactate also impaired mitochondrial function, determined by mPTP opening rate, mitochondrial membrane potential and mitochondrial biogenesis markers. Western blot analysis of LC3-II and p62 and mRFP-GFP-LC3 adenovirus detection for autophagy flux revealed that lactate blocked autophagy flux. LC3-II co-staining with LAMP-1 and autophagosome quantification revealed lactate inhibited autophagy. Furthermore, lactate inhibited mitophagy, which was confirmed by TOMM20 and BNIP3 protein levels, LC3-II colocalization with BNIP3 and TEM assays. In addition, BNIP3-mediated mitophagy played a protective role against VSMC calcification in the presence of lactate. This study suggests that lactate accelerates osteoblastic phenotype transition of VSMC and calcium deposition partly through the BNIP3-mediated mitophagy deficiency induced oxidative stress and apoptosis.

1. Introduction

Diabetic cardiovascular complications are the leading cause of high morbidity and mortality in diabetics [1]. Vascular calcification, an advanced atherosclerosis, occurs in the intima of blood vessels and vascular smooth muscle cells (VSMCs), the main cell type of vascular media, can lead to arterial media calcification through an osteoblastic phenotype transition under stress [2,3]. Several factors that cause vascular calcification in diabetic patients, including advanced glycation end products (AGEs) [3,4] and collagen receptor discoidin domain receptor 1 (DDR1) [5], have been found. However, the factors involved in vascular calcification still need further discovery. In clinical work, we found that patients with diabetes are usually accompanied by elevated levels of lactate, the end product of glycolysis; recent reports also support our findings [6–8]. During atherogenesis, VSMC will transdifferentiate from a contractile phenotype to a synthetic phenotype [9]. Lactate reportedly promotes the synthetic phenotype transition in VSMC [10]. Lactate can also induce osteoblast differentiation via hypoxia-inducible factor-1α (HIF-1α) [11]. Thus, we speculated that elevated levels of lactate and vascular calcification may have potential links.

Vascular calcification is currently considered an active, complex, and chronic process involving inflammation, oxidative stress, DNA damage response, autophagy, and apoptosis [12–15]. As a classic signaling pathway, the reactive oxygen species (ROS)/phosphatidylinositol-4,5-bisphosphate 3-kinase (PI3K)/protein kinase B (AKT)/nuclear factor kappa-light-chain-enhancer of activated B cells (NF-κB) axis plays a key role in vascular calcification [16,17]. The role of oxidative stress-induced apoptosis in VSMC calcification has been confirmed, apoptotic bodies serve as nucleation sites for calcium phosphate

Abbreviations: VSMC, vascular smooth muscle cell; ALP, alkaline phosphatase; RUNX2, runt-related transcription factor 2; BMP-2, bone morphogenetic protein 2; ROS, reactive oxygen species; mPTP, mitochondrial permeability transition pore; LC3-II, microtubule-associated protein 1 light chain 3B; p62, SQSTM1; LAMP-1, lysosomal-associated membrane protein 1; TOMM20, translocase of outer mitochondrial membrane 20; BNIP3, BCL2/adenovirus E1B 19 kDa protein-interacting protein 3; TEM, transmission electron microscope

* Corresponding author.
E-mail address: liunf@seu.edu.cn (N.-F. Liu).

https://doi.org/10.1016/j.cellsig.2019.03.006
Received 4 January 2019; Received in revised form 5 March 2019; Accepted 5 March 2019
Available online 06 March 2019
0898-6568/

precipitation [14]. Damaged mitochondria under stress are the main source of ROS formation [18,19], and then, removing impaired mitochondria should occupy the core position. Therefore, targeting excessive ROS generation is an important therapeutic approach for vascular calcification.

Mitophagy, a special form of autophagy that selectively eliminates damaged and unnecessary mitochondria, is stimulated as a protective mechanism by stress such as cellular ROS accumulation, mitochondrial swelling, mitochondrial membrane potential decline, and mitochondrial DNA damage [20,21]. Our team recently discovered metformin can attenuate VSMCs calcification via restoring mitochondrial biogenesis, and mitophagy is involved [22]. Frauscher, B., et al. reported autophagy induced by rapamycin protects cells and mice from uremic media calcification [23]. Our team also found that autophagy attenuates AGEs-stimulated VSMCs calcification, which is unpublished. Although inordinate autophagy also leads to apoptosis [24], appropriate autophagy and mitophagy induction may contribute to the alleviation of vascular calcification.

Although the relationship between lactate and mitophagy has not been reported yet, there have been a few reports on the connection between lactate, autophagy, and apoptosis. Tumor-derived lactate can suppress autophagy, eventually leading to cell apoptosis [25]. On the contrary, lactate treatment promotes apoptosis and autophagy in rat nucleus pulposus cells [26]. Lactate can also induce apoptosis in cardiomyocyte, intracellular ROS generation and the loss of mitochondrial membrane potential [27]. To a certain extent, the abnormal accumulation of lactate has been reported to cause metabolic disorders, especially in the presences of high oxidative stress and apoptosis induced by glycolipid metabolism disorder [28–30]. Based on previous studies, we speculated that lactate, mitophagy, ROS generation, and apoptosis are related, and the latter three are closely linked with vascular calcification.

In this study, we investigated the characteristics and potential mechanisms of lactate in vascular calcification through in vitro experiments. We found that lactate accelerates VSMC calcification partly through mitochondrial dysfunction, excessive intracellular ROS generation and, apoptosis. Furthermore, lactate inhibited autophagy flux and BNIP3-mediated mitophagy and up-regulated mitophagy significantly suppressed the ability of lactate to exacerbate VSMC calcification.

2. Materials and methods

2.1. Ethics statement

All animal studies were approved by the Ethics Committee of Southeast University and were performed in accordance with the Guidelines for the Care and Use of Laboratory Animals published by the China National Institutes of Health.

2.2. Cell culture

Primary VSMCs were isolated from six-week-old Sprague Dawley rat thoracic aortas (Experimental Animal Centre, Southeast University, Nanjing, China) according to previous protocols. VSMCs between passages 4 and 8 were incubated in a 1:1 mixture of Dulbecco's Modified Eagle's Medium (DMEM) and Ham's F12 medium with 10% fetal bovine serum and antibiotics at 37 °C with 5% CO_2. VSMC calcification was induced with 10 mM β-glycerophosphate (β-GP) according to previous protocols [3].

2.3. Cell viability analysis

VSMCs were seeded into 96-well plates at a density of 5000 cells/well and incubated for 24 h. The VSMCs were divided into the following 5 groups: control, β-GP (Sigma-Aldrich, St. Louis, MO, USA), β-GP + lactate (5 mM) (Sigma-Aldrich, St. Louis, MO, USA), β-GP + lactate (10 mM), and β-GP + lactate (15 mM). Then, each group was incubated for 12, 24, 48, and 72 h. After treatment, 10 μL of CCK-8 reagent (Beyotime Biotechnology, Jiangsu, China) was added to each well and cultured for 1–4 h at 37 °C. The absorbance was measured at a wavelength of 450 nm.

2.4. Measurement of the calcium content and ALP activity

The calcified VSMCs were decalcified with 0.6 M HCl for 24 h at 37 °C, and then the cells were washed twice with PBS and solubilized with 0.1 M NaOH containing 0.1% SDS. The calcium content in the VSMCs was measured using the Calcium Assay kit (Nanjing Jiancheng Bioengineering Institute, Nanjing, China) and normalized to the total protein content with a Bicinchoninic Acid (BCA) Protein Assay kit (KeyGEN Biotechnology, Jiangsu, China).

For ALP activity measurement, the calcified VSMCs were solubilized with RIPA lysis buffer (Beyotime Biotechnology, Jiangsu, China). After centrifugation, the supernatants were examined with the ALP activity kit (Nanjing Jiancheng Bioengineering Institute, Nanjing, China) and normalized to the total protein content.

2.5. Alizarin red S staining

The calcified VSMCs were fixed in 4% paraformaldehyde for 30 min at room temperature, washed twice with PBS, and then stained with 2% Alizarin red S (pH 8.4) (ScienCell Research Laboratories, Shanghai, China) for another 30 min at 37 °C. Excess Alizarin red S reagent was removed by washing with PBS. The calcium nodules were observed under a microscope.

2.6. Intracellular ROS detection

The intracellular ROS levels were detected using the oxidation-sensitive fluorescent probe dihydroethidium (DHE) (Beyotime Biotechnology, Jiangsu, China). After washing twice with serum-free DMEM, the VSMCs were incubated in the dark with 10 μM DHE for 30 min. Fluorescent DHE images were captured using a confocal microscope (FV10i, Olympus, Japan).

2.7. Measurement of superoxide dismutase (SOD) activity and the malondialdehyde (MDA) content

VSMCs were lysed with RIPA lysis buffer, and then the SOD activity and MDA content in the cell lysis buffer were measured according to the manufacturer's protocols (Beyotime Biotechnology, Jiangsu, China) and normalized to the total protein content.

2.8. TUNEL assays

The transferase-mediated dUTP nick-end labeling (TUNEL) method was performed with a detection kit (Roche, Germany) following the manufacturer's instructions. VSMCs were fixed with 4% paraformaldehyde at room temperature, washed twice with PBS, and then permeabilized with 0.1% Triton X-100 for FITC end labeling of the fragmented DNA of the apoptotic VSMCs. The TUNEL-positive cells were measured using confocal microscopy.

2.9. Mitochondrial function analysis

mPTP opening was measured based on a mPTP colorimetric detection kit (Genmed Scientifics Inc., Shanghai, China). The relative fluorescence units (RFUs) of mitochondrial volume changes were recorded by a spectrophotometer (MULTISKAN GO, Thermo Fisher Scientific, USA).

Mitochondrial membrane potential was evaluated via JC-1 staining

(KeyGEN Biotechnology, Jiangsu, China) by flow cytometry (BD Biosciences, USA). VSMCs with healthy mitochondria are distributed in Q2, while VSMCs with mitochondrial membrane potential decline are distributed in Q3.

The adenosine triphosphate (ATP) levels in the VSMCs were detected using an ATP assay kit (Beyotime Biotechnology, Jiangsu, China) according to the protocol. Luminescence was measured using a microplate reader (Bio-Rad, Shanghai, China).

2.10. Transfection

To overexpress BCL2/adenovirus E1B 19 kDa protein-interacting protein 3 (BNIP3), a LV-BNIP3 lentiviral vector was produced with puromycin-resistant genes (Shanghai Genechem Co., Ltd.). VSMCs were seeded into 6-well plates. The cells were transfected with the lentivirus (MOI = 5, 10, 15, 20, 25, and 30) when they were 30–40% confluent. Stable single clones were selected after 2 weeks of puromycin treatment (2 μg/μL). The transfection efficiency was evaluated using western blotting.

To silence Atg5, small interfering RNAs (siRNAs) were designed (Shanghai Genechem Co. Ltd.). The siRNAs were transfected into cells using Lipofectamine 2000 (Invitrogen Life Science, Grand Island, NY) according to the manufacturer's protocol. After 48 h of transfection, the silencing efficiency was examined by western blotting.

To detect the autophagic flux, VSMCs were transfected with a mRFP-GFP-LC3 double-labeled adenovirus (Shanghai Hanbio Biotechnology Co., Ltd.) for 5 h (MOI = 5). Then, the medium was renewed with complete medium. At 48 h after transfection, autophagosomes (yellow dots) and autolysosomes (red dots) were detected under a confocal microscope.

2.11. qRT-PCR

Total RNA was isolated using the TRIzol reagent (Biosharp, Anhui, China) according to the manufacturer's instructions. The RNA purity was evaluated based on the A260/A280 ratio using the Merinton SMA4000 system. Reverse transcription (RT) was performed with Prime Script™ Master Mix (Takara). Quantitative reverse transcriptase–polymerase chain reaction (qRT-PCR) was performed on a StepOnePlus system (ABI) using the SYBR Green Mix. The PCR primers are listed in Table 1. All mRNA expression levels were normalized to the β-actin expression level.

2.12. Western blotting analysis

The VSMCs were lysed according to the manufacturer's instructions, and the protein concentration was measured using the BCA Protein Assay kit. Antibodies against microtubule-associated protein 1 light chain 3 (LC3) (CST4108) (1:2000), SQSTM1 (p62) (CST23214) (1:500), cleaved caspase-3 (CST9661) (1:1000), cleaved caspase-9 (CST9509) (1:1000), Bcl-2 (CST3498) (1:1000), and Bax (CST14796) (1:1000) were obtained from Cell Signaling Technology (Danvers, MA, USA). Anti-runt-related transcription factor 2 (RUNX2) (ab76956) (1:1000), anti-bone morphogenetic protein 2 (BMP-2) (ab214821) (1:1000), anti-BNIP3 (ab109362) (1:1500), anti-pro caspase-3 (ab32499) (1:10000), anti-pro caspase-9 (ab135544) (1:500), anti-Atg5 (ab108327) (1:2000), and anti-translocase of outer mitochondrial membrane 20 (TOMM20) (ab186734) (1:500) antibodies were purchased from Abcam (Cambridge, MA, USA). Anti-β-actin (1:3000) and all secondary antibodies (1:5000) were provided by Biosharp (Anhui, China). Subsequently, 40–60 μg of protein was loaded onto a SDS-PAGE gel and then transferred onto nitrocellulose membranes. The membranes were blocked with 5% nonfat milk for 1.5 h. The membranes were incubated with different primary antibodies overnight at 4 °C and then visualized using anti-rabbit or anti-mouse IgG conjugated with horseradish peroxidase for 1 h at room temperature. The blots were detected using electrochemiluminescence (ECL), and the results were quantified with the Image-Pro Plus 6.0 software.

Table 1
Primer sequences for the qRT-PCR analysis.

Genes	Primer sequences
NRF-1	Forward, 5′-CTGGCTGAAGCCACCTTACA-3′ Reverse, 5′-ACTCCATCTGGGCCATTAGC-3′
PGC-1α	Forward, 5′-TTGACTGGCGTCATTCAGGA-3′ Reverse, 5′-CCAGGGCAGCACACTCTATG-3′
TFAM	Forward, 5′-AGTGATCTCATCCGTCGCAG-3′ Reverse, 5′-GTGCCCAATCCCAATGACAAC-3′
β-actin	Forward, 5′-GGCTGTATTCCCCTCCATCG-3′ Reverse, 5′-CCAGTTGGTAACAATGCCATGT-3′

2.13. Immunofluorescence staining

TVSMCs were fixed with 4% paraformaldehyde, permeabilized with 0.1% Triton X-100 for 20 min, and then blocked with 5% bovine serum albumin (BSA) for 0.5 h at room temperature. The cells were incubated with anti-LC3 (1:500), anti-lysosomal-associated membrane protein 1 (LAMP1) (ab24170) (1:500), anti-BNIP3 (1:500), and anti-RUNX2 (1:500) antibodies at 4 °C overnight, followed by the appropriate secondary antibodies for 0.5 h in the dark. The nuclei were stained with DAPI for 15 min. The images were visualized using a confocal microscope, and the results were quantified with the Image-J software.

2.14. Transmission electron microscopy (TEM)

The VSMCs were fixed in 2.5% glutaraldehyde (electron microscopy grade) at 4 °C for 2 h, dehydrated in an ethanol series, and embedded in Epon resin. Representative areas were chosen for ultrathin sections and viewed with a Hitachi TEM system at an accelerating voltage of 80 kV. Digital images were obtained by an AMT imaging system (Advanced Microscopy Techniques Co., Danvers, MA, USA).

2.15. Statistical analysis

All experiments were independently repeated at least three times. All data are presented as the mean ± standard deviation (SD). The statistical analyses were performed using the Statistical Package for Social Science (SPSS) 22.0 software (SPSS, Chicago, IL, USA). Two-tailed Student's *t*-tests and one- or two-way ANOVA with post hoc comparisons by Tukey's multiple comparisons test were used to compare the results. Values of $P < .05$ were considered statistically significant.

3. Results

3.1. Lactate accelerated calcification in VSMCs

As mentioned above, the VSMCs were divided into the following 5 groups for the cell viability analysis: control, β-GP, β-GP + lactate (5 mM), β-GP + lactate (10 mM), and β-GP + lactate (15 mM). As shown in Fig. 1A, the first 4 groups showed no significant effects on cell viability at different time points (12, 24, 48, and 72 h) and were applied for the subsequent experiments. In addition, to eliminate the effect of an acidic environment on the cell calcification evaluation, we measured the pH value and found no significant difference in the pH value among the groups (Supplementary Fig. 1).

Then, we cultured normal or calcified VSMCs with or without lactate treatment. Since BMP-2 and its downstream regulator RUNX2 (an important transcription factor) are both involved in VSMC osteoblastic differentiation [31,32], we chose BMP-2 and RUNX2 as detection markers. Lactate significantly increased the RUNX2 and BMP-2 protein

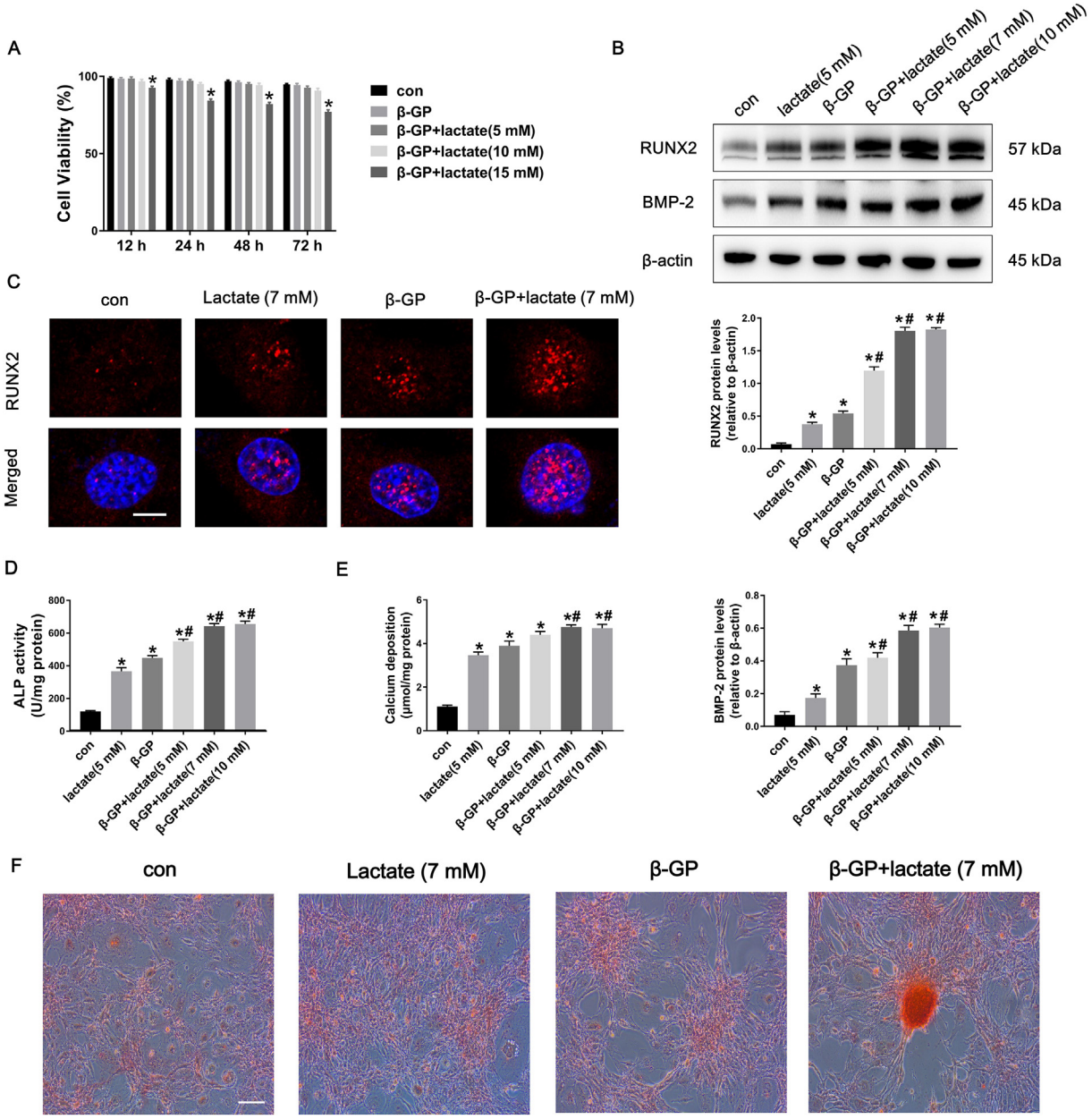

Fig. 1. Lactate accelerated VSMC osteoblastic phenotype transition and calcium deposition. (A) VSMCs were divided into 5 groups: control, β-GP, β-GP + lactate (5 mM), β-GP + lactate (10 mM), and β-GP + lactate (15 mM) group, then each group was incubated for 12, 24, 48, and 72 h. The cell viability was evaluated by CCK-8 assay. $^{*}P < .05$ compared with the control group at each time point (B) Normal or calcified VSMCs were incubated with or without lactate (5 mM, 7 mM and 10 mM) for 24 h. RUNX2 and BMP-2 expression were determined by western blotting. (C) After 24 h lactate (7 mM) treatment, RUNX2 nuclear translocation was evaluated by immunofluorescence with the confocal microscopy. At least 10–15 cells per condition were imaged. Scale bar, 5 μm. (D and E) ALP activity and calcium deposition were detected after 7 days intervention. $^{*}P < .05$ compared with the normal control group. $^{\#}P < .05$ compared with the β-GP group. (F) Normal or calcified VSMCs were incubated with or without lactate (7 mM) treatment for 21 days. Calcium nodule formation was visualized by Alizarin red S staining. At least 3–5 images per condition were imaged. Scale bar, 50 μm. Data are presented as the mean ± standard deviation of three experiments. (For interpretation of the references to colour in this figure legend, the reader is referred to the web version of this article.)

levels in normal or calcified VSMCs after 24 h of treatment. We also found that the effect of lactate on normal VSMC osteogenic differentiation was close to that of the calcification model (Fig. 1B). To further clarify the association between RUNX2 and lactate, normal or calcified VSMCs were incubated with or without lactate for 24 h, and the cellular RUNX2 distributions were visualized by immunofluorescence staining. The images indicated that lactate significantly promoted RUNX2 translocation into the nuclei compared with that of the control and β-GP groups (Fig. 1C), suggesting regulation at the transcriptional level. In addition, lactate treatment increased ALP activity and the calcium deposition content after 7 days of intervention (Fig. 1D and E). Calcified nodule formation was also significant after 21 days in lactate culture (Fig. 1F). These results revealed that lactate played an important role in VSMC calcification.

3.2. Lactate-induced oxidative stress and apoptosis during VSMC calcification

To explore whether lactate, oxidative stress, and cell apoptosis were inextricably linked during VSMC calcification, the calcified VSMCs were cultured with or without lactate for 24 h. High oxidative stress involves elevated intracellular ROS levels, and a high Pi level has been

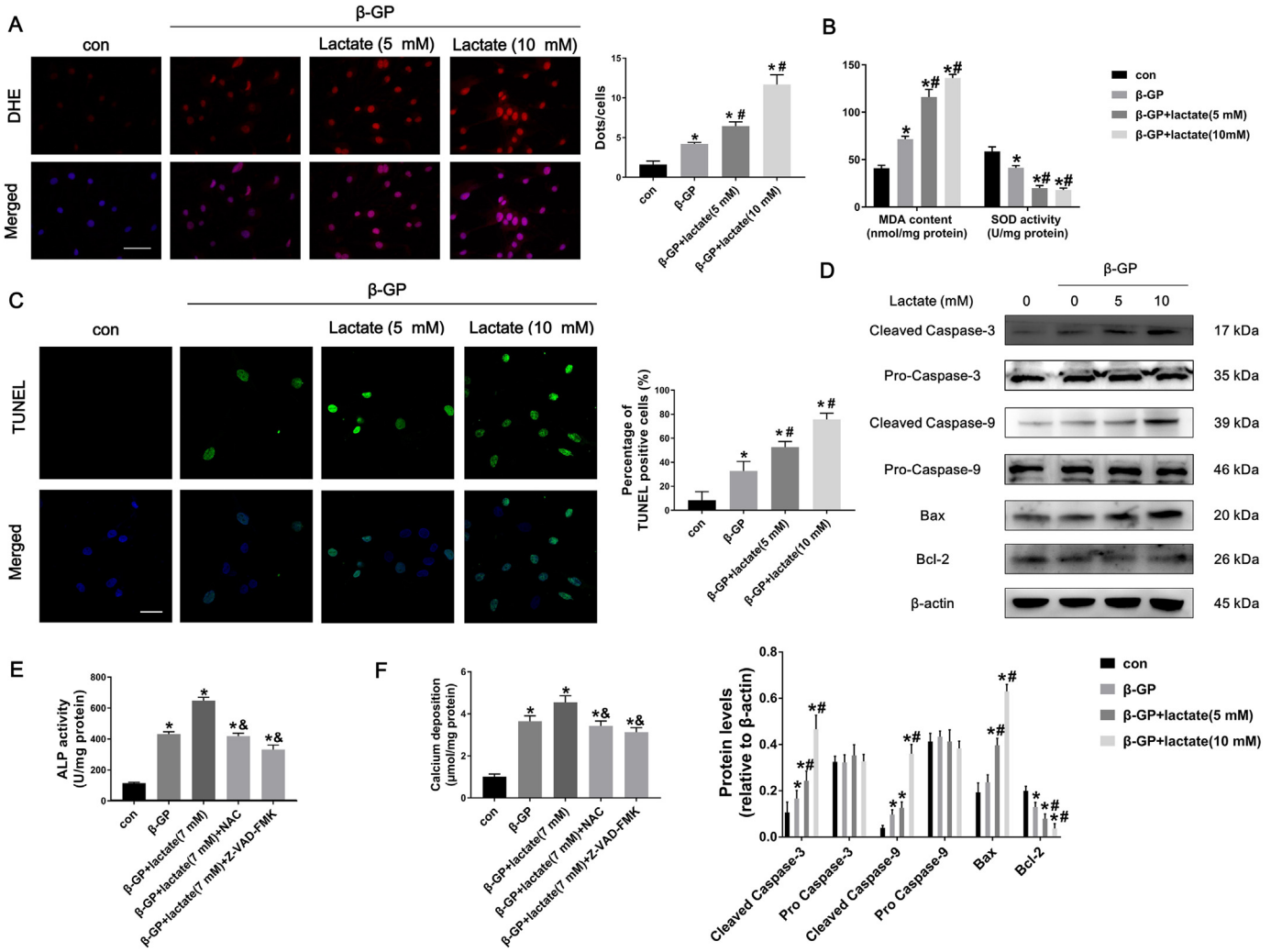

Fig. 2. Lactate caused oxidative stress and apoptosis during VSMC calcification. Normal or calcified VSMCs were incubated with or without lactate (5 mM and 10 mM) for 24 h. (A) ROS production was measured by immunofluorescence with the confocal microscopy. At least 3–5 images per condition were imaged. Scale bar, 50 μm. (B) SOD activity and MDA content were determined. $^{*}P < .05$ compared with the normal control group. $^{\#}P < .05$ compared with the β-GP group. (C) Representative photographs of TUNEL positive VSMC staining in the different groups. At least 5–7 images per condition were imaged. Quantification represents the percentage of TUNEL positive cells in each group. Scale bar, 20 μm. (D) Western blot analysis of Cleaved-caspase3, Cleaved-caspase9, Bcl-2, and BAX expression. (E and F) ALP activity and calcium deposition detection in the present of NAC or *Z*-VAD-FMK treatment. $^{*}P < .05$ compared with the normal control group. $^{\&}P < .05$ compared with the β-GP + lactate group. Data are presented as the mean ± standard deviation of three experiments.

reported to induce the production of mitochondrial superoxide anion and to activate NF-kB for the induction of vascular calcification [33]. As shown in Fig. 2A, DHE-positive cells were increased in the β-GP-treated groups compared with that of the control group. The addition of lactate further promoted intracellular ROS generation compared with that of the β-GP alone group. Furthermore, compared to that of the control or β-GP group, the MDA content was markedly increased in the β-GP + lactate group and the SOD activity was significantly decreased, indicating high oxidative stress levels (Fig. 2B). Because oxidative stress is linked to cell apoptosis, next we detected apoptosis in VSMCs after 24 h of lactate treatment. We determined that more TUNEL^{+} VSMCs were present in the lactate-treated group than in the control or β-GP group (Fig. 2C). Caspases play a central role in the regulation and execution of apoptosis; caspase3 stimulates the ultimate step in apoptosis, whereas BCL-2 and Bax are key regulators of apoptosis [34]. Incubation with lactate enhanced the pro-apoptosis protein levels (cleaved-caspase3, cleaved-caspase9, and Bax) but diminished anti-apoptosis protein expression (Bcl-2) (Fig. 2D). As expected, *N*-acetylcysteine (NAC) (antioxidant) or *Z*-VAD-FMK (apoptosis inhibitor) intervention in the presence of lactate decreased the ALP activity and calcium content (Fig. 2E).Therefore, these results demonstrated that intracellular ROS generation and apoptosis were involved in lactate-induced VSMC calcification.

3.3. Lactate impaired mitochondrial function and biogenesis in VSMCs

Mitochondria are the original sites for ROS production and are targets for oxidative damage [35]. When cells undergo stress and injury, the mPTP opens, leading to a membrane potential decline [36]. In our study, normal or calcified VSMCs were cultured with or without lactate for 24 h. Calcified VSMCs presented an increased rate of mPTP opening, and lactate treatment enhanced this effect to a high degree (Fig. 3A). Using JC-1 staining, more mitochondria are distributed in Q3 after lactate exposure than those in the control or β-GP group, suggesting an aggravated decline in the mitochondrial membrane potential (Fig. 3B). Mitochondria are the factories of energy currency of the cell. Our results suggested that lactate could down-regulate the β-GP-induced decrease in intracellular ATP production (Fig. 3C), revealing a destructive role for lactate in mitochondrial dysfunction.

Next, we examined the mRNA expression levels of the

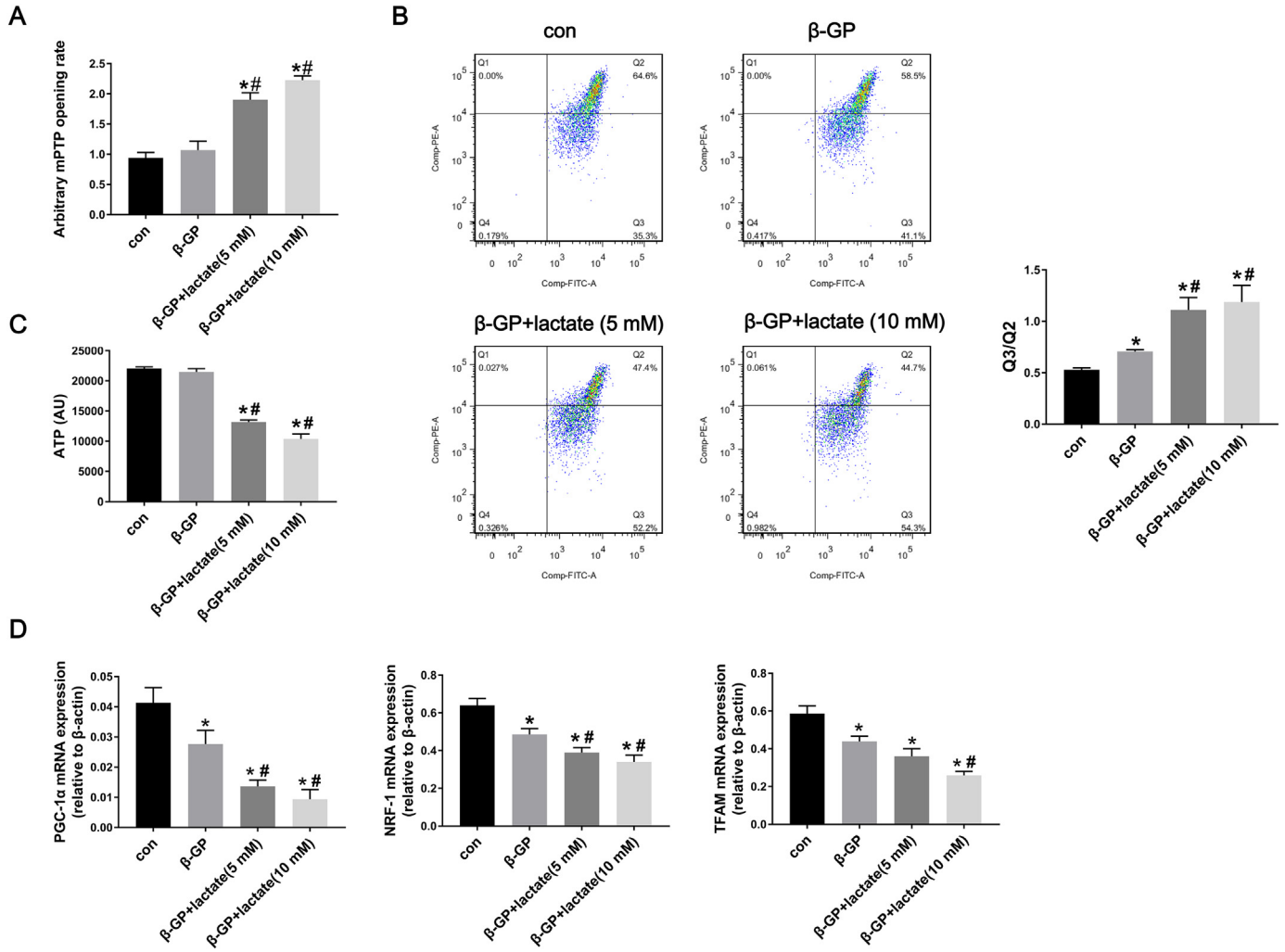

Fig. 3. Lactate induced mitochondrial dysfunction during VSMC calcification. Normal or calcified VSMCs were cultured with or without lactate (5 mM and 10 mM) for 24 h. (A) The RFU of mPTP opening was evaluated by spectrophotometry at 505 nm. (B) The mitochondrial membrane potential was measured via JC-1 staining with flow cytometry. (C) Intracellular ATP levels were detected. (D) The mRNA expression of mitochondrial biogenesis markers. $^{*}P < .05$ compared with the normal control group. $^{\#}P < .05$ compared with the β-GP group. Data are presented as the mean ± standard deviation of three experiments.

mitochondrial biogenesis markers, peroxisome proliferator-activated receptor gamma coactivator 1-alpha (PGC-1α), nuclear respiratory factor 1 (NRF-1), and mitochondrial transcription factor A (TFAM). All these markers, which are important for the replication of mitochondrial DNA and the transcription of nuclear-encoded genes [37], were down-regulated in the calcified VSMCs, and lactate treatment decreased the mRNA levels of the three markers significantly (Fig. 3D). These results suggested that lactate further disturbed mitochondrial homeostasis of VSMCs in calcium medium.

3.4. Lactate suppressed the autophagic flux and mitophagy in VSMCs

Since we found that lactate caused mitochondrial dysfunction and a biogenesis deficiency, next we explored the relationship between lactate and mitophagy to examine the condition of damaged mitochondrial clearance. First, we evaluated the autophagic flux. In calcified VSMCs, the LC3-II protein level was increased and p62 was decreased compared with those of the control group. However, after lactate treatment for 24 h, the trend of LC3-II and p62 expression was reversed (Fig. 4A), indicating an autophagic flux block. To further determine alterations in the autophagic flux, normal or calcified VSMCs were transfected with the mRFP-GFP-LC3 adenovirus and then treated with or without lactate for 24 h. We found that the numbers of both GFP (green) and mRFP (red) dots were increased in the calcified VSMCs and that more yellow and red dots were present, indicating an increase in the formation of both autophagosomes and autolysosomes. However, after lactate treatment, only yellow, but not red, dots were found, suggesting that the autophagosomes were not degraded by lysosomes. We then used lysosomal inhibitor chloroquine (CQ) (10 μM) (C6628, Sigma) and siRNA against Atg5 (the silencing efficiency was almost 80%, Supplementary Fig. 2A) in conjunction with lactate to prevent autolysosomes formation. We found that the raito of autolysosomes/autophagosomes in the CQ or si-Atg5 group further decreased compared with the lactate or scrambled siRNA groups (Fig. 4B). Western blot analysis of LC3-II and p62 protein levels was used as a positive control (Supplementary Fig. 2B). Thus, coupling the pharmacological inhibition of autophagy with the genetic silencing of Atg5 gave conclusive evidence of lactate in mediating autophagic flux. To examine whether lactate could block autophagosome and lysosome fusion, LC3-II and LAMP1 were co-stained. After incubation with lactate, the extent of colocalization was lower than that of the control or β-GP group (Fig. 4C). The TEM assay also demonstrated that the number of autophagosomes was reduced in the lactate-treated group compared with that of the control or β-GP group (Fig. 4D). Therefore, these results suggested that lactate could block the autophagic flux. Autophagy and apoptosis both act as programmed cell death (PCD), and complex interactions exist between the

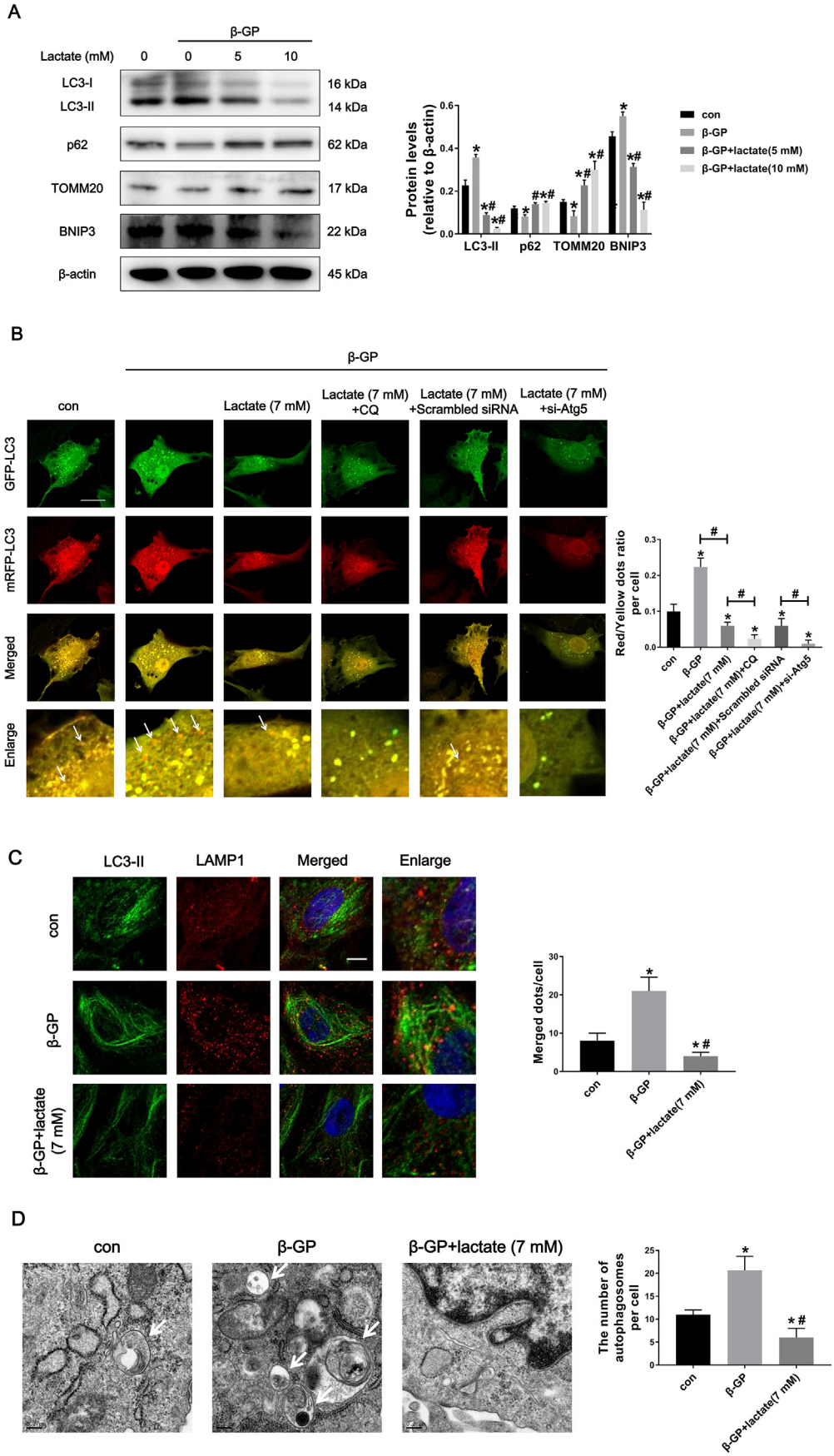

Fig. 4. Lactate blocked autophagy flux during VSMC calcification. (A) After 24 h lactate (5 mM and 10 mM) treatment in normal or calcified VSMCs, LC3-II/I, p62, TOMM20, and BNIP3 protein levels were evaluated by western blotting. $^{*}P < .05$ compared with the normal control group. $^{\#}P < .05$ compared with the β-GP group. (B) VSMCs were treated with CQ (10 μM) for 12 h or transfected with siRNA against Atg5 and scrambled siRNA for 48 h. Fluorescent analysis of calcified VSMCs transfected with mRFP-GFP-LC3 adenovirus and then treated with or without lactate (7 mM) for 24 h. The yellow puncta indicate autophagosomes, and the free red puncta indicate autolysosomes (white arrows). Scale bar, 20 μm. At least 8–10 cells per condition were imaged. Quantification represents the ratio of autolysosome/autophagosome in each group. $^{*}P < .05$ compared with the normal control group. $^{\#}P < .05$ vs. the indicated treatment. (C) Immunofluorescent images double labeled by LC3-II (green) and LAMP1 (red). At least 8–10 cells per condition were imaged. Scale bar, 5 μm. $^{*}P < .05$ compared with the normal control group. $^{\#}P < .05$ compared with the β-GP group. (D) Representative TEM photomicrographs showing the formation of autophagosomes containing organelles fragments (white arrows). At least 8–10 cells per condition were imaged. Quantification represents the number of autophagosomes in each group. Scale bar, 0.2 μm. $^{*}P < .05$ compared with the normal control group. $^{\#}P < .05$ compared with the β-GP group. Data are presented as the mean ± standard deviation of three experiments. (For interpretation of the references to colour in this figure legend, the reader is referred to the web version of this article.)

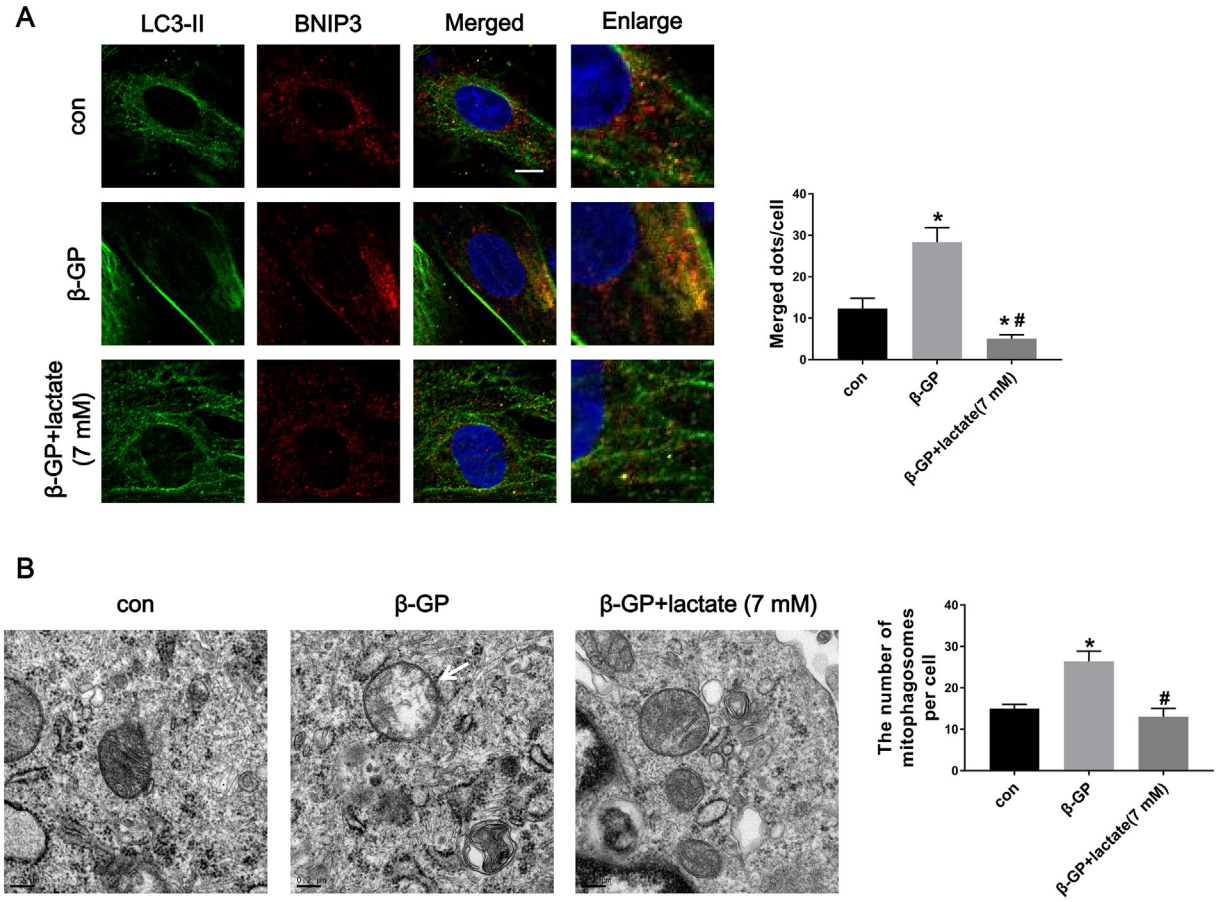

Fig. 5. Lactate inhibited mitophagy in VSMC. (A) After 24 h lactate (7 mM) treatment, VSMCs were double stained by LC3-II (green) and BNIP3 (red). At least 8–10 cells per condition were imaged. Scale bar, 5 μm. (B) Representative photomicrographs displaying the formation of mitophagosomes containing mitochondria fragments (white arrows) were detected by TEM. At least 8–10 cells per condition were imaged. Quantification showed that the number of mitophagosomes was lowered by lactate treatment. Scale bar, 0.2 μm. $^{*}P < .05$ compared with the normal control group. $^{\#}P < .05$ compared with the β-GP group. Data are presented as the mean ± standard deviation of three experiments. (For interpretation of the references to colour in this figure legend, the reader is referred to the web version of this article.)

two pathways; for instance, they can be activated by multiple stressors, share multiple regulatory molecules, and even coordinate with each other [38]. To rule out the effects of excessive lactate-induced apoptosis on the autophagic levels, we interfered calcified VSMCs with *Z*-VAD-FMK after lactate treatment and observed that both the LC3-II and p62 protein levels were unchanged statistically (Supplementary Fig. 3), indicating that lactate directly inhibited autophagy in VSMCs.

Next, we investigated the changes in mitophagy after lactate incubation. The lower TOMM20 (a translocase of the outer mitochondrial membrane) protein levels induced by β-GP were increased after incubation with lactate, indicating attenuated mitochondrial clearance (Fig. 4A). In addition, lactate treatment inhibited LC3-II and BNIP3 fusion compared with that of the control or β-GP group (Fig. 5A). The TEM assay was used to provide directly evidence of mitophagy. As shown in Fig. 5B, the number of autophagosomes with double-membrane structures containing swelled and dilated mitochondria (white arrows) was decreased in the β-GP + lactate group. Thus, we concluded that lactate suppressed β-GP-induced autophagy and mitophagy, resulting in an inability to remove damaged mitochondria.

3.5. BNIP3-mediated mitophagy reversed mitochondrial disorder and excessive oxidative stress

The role of mitophagy in anti-oxidative stress has been well established [39], but its relationship with mitochondria is influenced by the cell type, duration of action, and intensity of autophagy. We discussed only the role of mitophagy in lactate-induced mitochondrial damage here. We focused on BNIP3-mediated mitophagy. Lactate inhibited BNIP3 expression (Fig. 4A). To overexpress BNIP3, the VSMCs were transfected with a lentivirus against BNIP3 or an empty vector; the transfection efficiency was approximately 70% according to the western blotting analysis (Supplementary Fig. 4). BNIP3 overexpression and uncoupler carbonyl cyanide *m*-chlorophenyl hydrazone (CCCP) (an inducer of mitophagy) not only promoted mitochondrial biogenesis (Fig. 6A) but also attenuated the mitochondrial dysfunction determined by the mPTP opening rate and mitochondrial membrane potential (Fig. 6B and C). Although CCCP is a mitochondrial electron transport chain inhibitor, we speculated that autophagic compensation after mitochondrial injury could offset the damage effect of CCCP on mitochondria over a short time period. Furthermore, activation of mitophagy reduced the MDA content but increased the SOD activity (Fig. 6D). In summary, mitophagy played a protective role against mitochondrial injury under lactate by controlling the source of ROS generation.

3.6. BNIP3-mediated mitophagy attenuated lactate-induced VSMC calcification

We discovered that BNIP3-induced mitophagy played an anti-oxidative stress role. Therefore, we explored whether BNIP3-mediated mitophagy could suppress the osteoblastic phenotype transition of VSMCs and calcium deposition. The western blotting analysis indicated

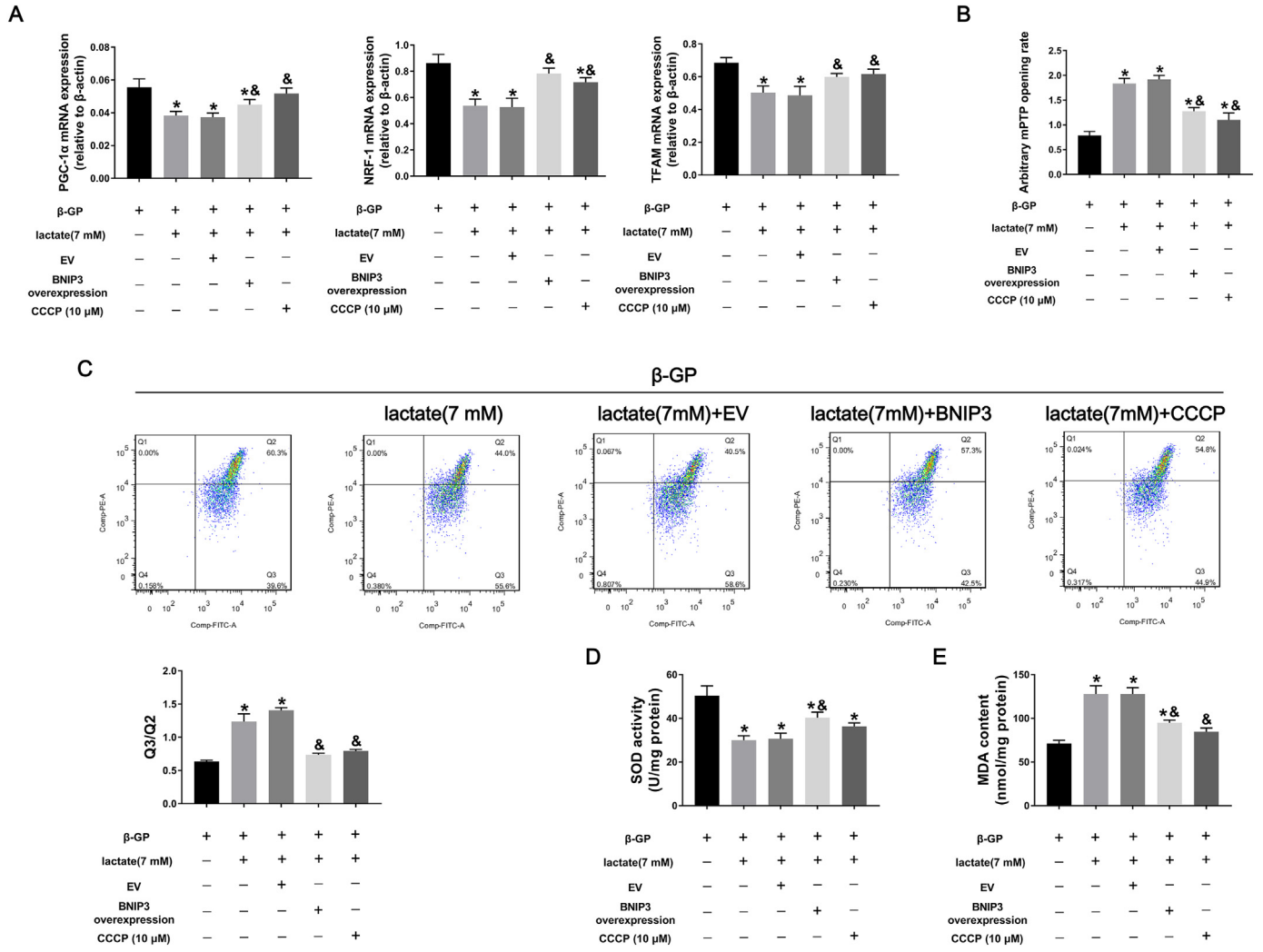

Fig. 6. Mitophay preserved mitochondrial function, biogenesis and oxidative stress. (A) Enhanced mitophagy was induced by a lentivirus against BNIP3 transfenction or 20 min CCCP (10 μM) treatment, then calcified VSMCs were treated with or without lactate (7 mM) for 24 h. The mRNA expression of mitochondrial biogenesis markers were determined by qRT-PCR. (B) mPTP opening rate detection. (C) The mitochondrial membrane potential measurement via JC-1 staining with flow cytometry. (D and E) After 7 days culture, the ALP activity and calcium deposition were evaluation. $^{*}P < .05$ compared with the normal control group. $^{\&}P < .05$ compared with the β-GP + lactate group. Data are presented as the mean ± standard deviation of three experiments.

that BNIP3 overexpression or CCCP treatment down-regulated RUNX2 and BMP-2 expression compared with that of the β-GP + lactate group (Fig. 7A). ALP activity and the calcium content measurement also showed an opposing role of mitophagy on calcium deposition after 72 h of intervention with lactate (Fig. 7B and C). Furthermore, enhanced mitophagy markedly decreased lactate-induced calcified nodule formation, as shown by Alizarin red S staining (Fig. 7D). These data revealed that mitophagy could suppress lactate-induced VSMC calcification.

4. Discussion

We explored the characteristics and a potentially novel mechanism of lactate in VSMC calcification. There are three main findings presented in this work. First, we observed that lactate treatment accelerates VSMC calcification through mitochondrial dysfunction, which is related to excessive intracellular ROS generation and apoptosis. Second, there is a tight link between lactate, autophagy and mitophagy. Enhanced autophagy and mitophagy existed under calcium medium as a compensation mechanism. However, lactate suppressed the balance of mitochondrial injury and clearance. Third, mitophagy inhibited lactate-induced VSMC calcification by attenuating mitochondrial disorder and oxidative stress; this was especially seen in BNIP3-mediated mitophagy. Therefore, interventions focusing on circulating lactate levels in diabetic patients may serve as a novel therapeutic target in vascular calcification, as well as the function of mitochondrial homeostasis in managing diabetic vascular complications.

Vascular calcification and adverse cardiovascular events are strongly correlated [40]. Coronary artery calcification has been reported as a predictor of adverse cardiac events in asymptomatic patients [41]. Coronary artery calcium (CAC) score, a non-traditional risk factor of cardiovascular disease (CVD), is also beneficial for clinical evaluations [42]. It is essential to effectively prevent vascular calcification to manage CVD. Glucose metabolism research has become increasingly important in CVD research. Glucose metabolism is the main breakthrough in VSMC energy acquisition. Approximately 30% of the ATP supply in VSMCs is derived from aerobic glycolysis, and almost 90% of the glycolysis flux contributes to lactate production [43]. Glucose metabolism impairment or collapse is involved in CVD pathogenesis, including vascular calcification [3,44,45]. Lactate accumulation causes a disturbed glucose metabolism. In addition, pyruvate dehydrogenase kinase 4 (PDK4), an important mitochondrial matrix enzyme in cellular metabolism shift, plays an important role in accelerating vascular calcification [3,22,46]. An abnormal rise in PDK4

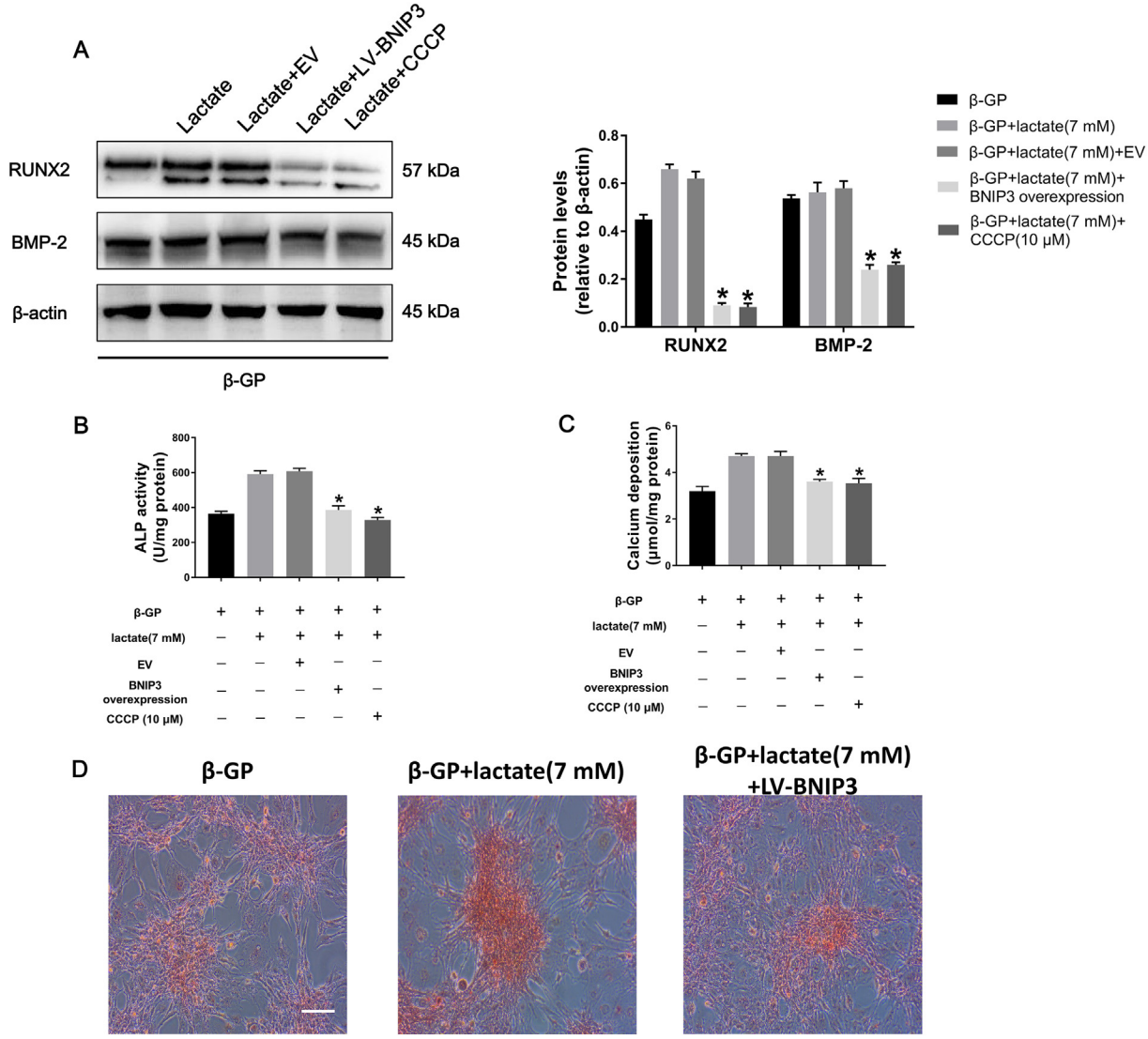

Fig. 7. BNIP3-mediated mitophagy reversed lactate-induced VSMC calcification. (A) After lentivirus against BNIP3 transfenction or CCCP (10 μM) treatment, calcified VSMCs were treated with or without lactate (7 mM) for 24 h, then RUNX2 and BMP-2 protein levels were measured by western blotting. (B and C) After 7 days culture, ALP activity and calcium deposition were determined. (D) Calcium nodule formation was visualized by Alizarin red S staining on the 21st day. At least 3–5 images per condition were imaged. Scale bar, 50 μm. $^{*}P < .05$ compared with the β-GP + lactate group. Data are presented as the mean ± standard deviation of three experiments. (For interpretation of the references to colour in this figure legend, the reader is referred to the web version of this article.)

levels leads to massive accumulation of lactate [3]. Based on the above research, we explored the link between lactate and VSMC calcification. We measured the concentration of lactate in VSMC medium, after 24 h. of non-liquid exchange culture, the lactate concentration in the common culture medium is 3.5 mM, while the calcification medium is 6 mM. This phenomenon may be related to the glucose metabolism impairment in the calcification medium, and gives a reference range of concentration for our lactate intervention. We were the first to observe appropriate concentrations of lactate accelerate β-GP-induced calcification in VSMCs, providing evidence for future research on lactate levels for vascular lesion assessment.

The main part we intended to demonstrate in our study was the potential molecular mechanisms of osteoblastic phenotype transition of VSMC. Excessive oxidative stress exists as a key point in diabetic vascular complications [47]. We previously reported that AGEs accelerate VSMC calcification through oxidative stress pathway [48]. ROS are signal molecules in oxidative stress that play an important role in cellular growth and function [49]. However, excessive ROS generation can accelerate VSMC apoptosis [50], which is also implicated in diabetic vascular calcification [14]. In our study, lactate treatment enhanced oxidative stress and VSMC apoptosis, further supporting that lactate accelerates vascular calcification.

As a central regulatory role of energy metabolism, mitochondrial dysfunction results in an imbalance between inflammation and the elimination of ROS. This ultimately triggers apoptotic cell death. Moreover, the damage to the mitochondria itself increases the permeability of the mitochondrial membrane, causing cytochrome C to be released and stimulate the mitochondrial apoptotic pathway [51,52]. We measured the changes of mPTP opening rate, mitochondrial membrane potential and mitochondrial biogenesis. We observed an increased mPTP opening rate, mitochondrial membrane potential decline and weakened mitochondrial biogenesis in calcified VSMCs, consistent with our previous study [22]. After lactate incubation, the changes were even more evident, thereby further accelerating ROS production and apoptosis. In recent years, mitophagy has become a hot field for CVD prevention and treatment. Mitophagy removes damaged mitochondria and maintains mitochondrial homeostasis, thereby fundamentally combating oxidative stress, which is impossible for many external interventions that simply resist oxidative stress [19,53]. At the same time, we found mitophagy can improve mitochondrial biogenesis,

control mitochondrial mass, and thus play an anti-apoptotic role [22]. In our study, we also found mitophagy activation can promote mitochondrial biogenesis. Excessive mitophagy in the absence of mitochondrial biogenesis may damage mitochondrial function [54] while the proper mitophagy level helps maintain the balance between the both. The levels of autophagy and mitophagy increased in high phosphate environments, thus counteracting internal environmental disorders. However, the addition of lactate not only aggravated mitochondrial damage, it also inhibited the compensatory mechanism, thus continuing to cause cell damage. Although the damaged VSMCs tend to accumulate lactate, the blood lactate level of most diabetic patients does not rise to the levels required in drug intervention, so the entry point can only be mitophagy.

Several reports have shown a protective role of autophagy against vascular calcification [55,56], but mitophagy research countering vascular calcification is still relatively rare. Three mechanisms of mitophagy have been widely investigated: BNIP3-related mitophagy, the PTEN-induced putative kinase 1 (PINK1)/parkin pathway, and FUN14 domain containing 1 (FUNDC1)-mediated mitophagy [18]. In addition to PINK1/parkin pathway [57], the association of the other two mitophagy pathways with lactate has not been reported. In this study, we focused on BNIP3-related mitophagy, BNIP3 interacts with LC3 family proteins via its LIR motifs facing the cytosol, thereby mediating mitophagy [58]. After lactate treatment, BNIP3 expression was downregulated, the fusion of BNIP3 and LC3 were also suppressed, indicating BNIP3-mediated mitophagy deficiency should be a part of lactate-induced VSMC calcification. As we expected, BNIP3 overexpression attenuated high levels of oxidative stress and vascular calcification, to some extent. However, BNIP3 also contributes to cell apoptosis through activation of the mitochondrial apoptotic pathway. The degree of mitophagy induced by BNIP3 is much higher than that of induced mPTP opening and cell death [59–61]. In our study, the autophagy enhancement played a protective role in vascular calcification, but excessive levels of autophagy also lead to apoptosis [62], aggravating the damage of VSMC and other cell components of the atherosclerosis plate, such as endothelial cells and macrophages. The large amount of inflammatory factors released also promotes vascular calcification deposition [63]. Autophagy presents as a double-edged sword. The specific and reasonable control range is interfered by many factors, and finer molecular regulation has become a hot research field. In addition, hypoxia plays an important role in glucose metabolism disorder, lactate accumulation, vascular calcification and other CVD complications; the latter two pathways of mitophagy are usually modulated by HIF-1α [64,65], and the relationship between lactate and the other two pathways requires further study.

Our study also has some limitations. The increase in lactate may affect the glucose enzymes metabolism, especially lactate dehydrogenase (LDH), which regulates HIF-1α [66], an important molecule in VSMC calcification [3]. The follow-up study will investigate the relationship between key enzymes of glucose metabolism and the VSMC phenotypic transformation. Furthermore, this study is only for in vitro VSMC studies. Diabetic vascular calcification mice may provide direct evidence for lactate metabolism and vascular calcification studies.

5. Conclusion

In summary, this study demonstrated that lactate accelerates VSMC calcification and contributes to mitochondrial dysfunction and mitochondrial biogenesis deficiency. These complications could cause excessive intracellular ROS generation and apoptosis. Lactate exaggerated mitochondrial injury by suppressing elevated autophagy and mitophagy of VSMCs under calcium medium. BNIP3-related mitophagy alleviated lactate-induced VSMC calcification. In the future, further precautions should be taken when managing blood lactate levels in diabetic patients and the protective effects of mitophagy could be a novel target for the treatment of diabetic vascular calcification.

Declaration of interest

The authors have no conflict of interest.

Author contributions

YZ was the principal investigator and was involved in the experimental design, biochemistry detection, data analysis, and writing of the manuscript. WQM, XQH, JJJ, SXJ, and YR contributed to the cell culture and the discussion. NFL provided expertise in experimental design.

Acknowlegements

This work was supported by the National Nature Science Foundation of China (No. 81770451).

Appendix A. Supplementary data

Supplementary data to this article can be found online at https://doi.org/10.1016/j.cellsig.2019.03.006.

References

[1] N.S. Asfandiyarova, Risk factors of death in diabetes mellitus, Klin. Med. (Mosk) 94 (9) (2016) 697–700.
[2] S. Disthabanchong, Phosphate and cardiovascular disease beyond chronic kidney disease and vascular calcification, Int. J. Nephrol. 2018 (2018) 3162806.
[3] Y. Zhu, et al., Advanced glycation end products accelerate calcification in VSMCs through HIF-1alpha/PDK4 activation and suppress glucose metabolism, Sci. Rep. 8 (1) (2018) 13730.
[4] Y. Wang, et al., Exosomes derived from mesenchymal stromal cells pretreated with advanced glycation end product-bovine serum albumin inhibit calcification of vascular smooth muscle cells, Front. Endocrinol. (Lausanne) 9 (2018) 524.
[5] M. Lino, et al., Diabetic vascular calcification mediated by the collagen receptor discoidin domain receptor 1 via the phosphoinositide 3-kinase/Akt/runt-related transcription factor 2 signaling axis, Arterioscler. Thromb. Vasc. Biol. 38 (8) (Aug 2018) 1878–1889.
[6] L. Zhao, et al., Metabolomic analysis identifies lactate as one important pathogenic factor in diabetes-associated cognitive decline rats, Mol. Cell. Proteomics 17 (12) (Dec 2018) 2335–2346.
[7] E.C. Wiegers, et al., Effect of lactate administration on brain lactate levels during hypoglycemia in patients with type 1 diabetes, J. Cereb. Blood Flow Metab. (May 11 2018) (271678X18775884).
[8] S.O. Crawford, et al., Association of blood lactate with type 2 diabetes: the Atherosclerosis Risk in Communities Carotid MRI Study, Int. J. Epidemiol. 39 (6) (2010) 1647–1655.
[9] C.M. Shanahan, P.L. Weissberg, Smooth muscle cell heterogeneity: patterns of gene expression in vascular smooth muscle cells in vitro and in vivo, Arterioscler. Thromb. Vasc. Biol. 18 (3) (1998) 333–338.
[10] L. Yang, et al., Lactate promotes synthetic phenotype in vascular smooth muscle cells, Circ. Res. 121 (11) (2017) 1251–1262.
[11] Y. Wu, et al., Lactate induces osteoblast differentiation by stabilization of HIF1alpha, Mol. Cell. Endocrinol. 452 (2017) 84–92.
[12] S.V. Suryavanshi, Y.A. Kulkarni, NF-kappabeta: a potential target in the management of vascular complications of diabetes, Front. Pharmacol. 8 (2017) 798.
[13] K.M. Lee, et al., APE1/Ref-1 Inhibits Phosphate-Induced Calcification and Osteoblastic Phenotype Changes in Vascular Smooth Muscle Cells, 18 (2017), p. 10.
[14] S. Koike, et al., Advanced glycation end-products induce apoptosis of vascular smooth muscle cells: a mechanism for vascular calcification, Int. J. Mol. Sci. 17 (9) (2016).
[15] J.A. Leopold, Vascular calcification: mechanisms of vascular smooth muscle cell calcification, Trends Cardiovasc. Med. 25 (4) (2015) 267–274.
[16] C.H. Byon, et al., Oxidative stress induces vascular calcification through modulation of the osteogenic transcription factor Runx2 by AKT signaling, J. Biol. Chem. 283 (22) (2008) 15319–15327.
[17] T. Pan, et al., Correction to: geniposide suppresses interleukin-1beta-induced inflammation and apoptosis in rat chondrocytes via the PI3K/Akt/NF-kappaB signaling pathway, Inflammation 42 (1) (Feb 2019) 404–405.
[18] Y. Zhao, et al., Mitophagy contributes to the pathogenesis of inflammatory diseases, Inflammation 41 (5) (2018) 1590–1600.
[19] A. Di Rita, et al., AMBRA1-mediated mitophagy counteracts oxidative stress and apoptosis induced by neurotoxicity in human neuroblastoma SH-SY5Y cells, Front. Cell. Neurosci. 12 (2018) 92.
[20] T. Saito, J. Sadoshima, Molecular mechanisms of mitochondrial autophagy/mitophagy in the heart, Circ. Res. 116 (8) (2015) 1477–1490.
[21] L. Liu, et al., Receptor-mediated mitophagy in yeast and mammalian systems, Cell Res. 24 (7) (2014) 787–795.
[22] W.Q. Ma, et al., Restoring mitochondrial biogenesis with metformin attenuates beta-GP-induced phenotypic transformation of VSMCs into an osteogenic

phenotype via inhibition of PDK4/oxidative stress-mediated apoptosis, Mol. Cell. Endocrinol. 479 (Jan 5 2018) 39–53.
[23] B. Frauscher, et al., Autophagy protects from uremic vascular media calcification, Front. Immunol. 9 (2018) 1866.
[24] J. Doherty, E.H. Baehrecke, Life, death and autophagy, Nat. Cell Biol. 20 (10) (2018) 1110–1117.
[25] H. Xia, W. Wang, Suppression of FIP200 and Autophagy by Tumor-derived Lactate Promotes Naive T Cell Apoptosis and Affects Tumor Immunity, 2 (2017), p. 17.
[26] W. Wu, et al., Lactate down-regulates matrix systhesis and promotes apoptosis and autophagy in rat nucleus pulposus cells, J. Orthop. Res. 32 (2) (2014) 253–261.
[27] C. Gao, et al., Asiatic acid inhibits lactate-induced cardiomyocyte apoptosis through the regulation of the lactate signaling cascade, Int. J. Mol. Med. 38 (6) (2016) 1823–1830.
[28] X. Sui, et al., miR-291b-3p mediated ROS-induced endothelial cell dysfunction by targeting HUR, Int. J. Mol. Med. 42 (5) (2018) 2383–2392.
[29] Z. Liu, et al., Resveratrol enhances cisplatin-induced apoptosis in human hepatoma cells via glutamine metabolism inhibition, BMB Rep. 51 (9) (2018) 474–479.
[30] H. Zhang, et al., PGC1beta regulates multiple myeloma tumor growth through LDHA-mediated glycolytic metabolism, Mol. Oncol. 12 (9) (2018) 1579–1595.
[31] Z.H. Wu, et al., DGCR5 induces osteogenic differentiation by up-regulating Runx2 through miR-30d-5p, Biochem. Biophys. Res. Commun. 505 (2) (Oct 28 2018) 426–431.
[32] W.L. Sun, N. Wang, Y. Xu, Impact of miR-302b on calcium-phosphorus metabolism and vascular calcification of rats with chronic renal failure by regulating BMP-2/Runx2/Osterix signaling pathway, Arch. Med. Res. 49 (3) (2018) 164–171.
[33] M.M. Zhao, et al., Mitochondrial reactive oxygen species promote p65 nuclear translocation mediating high-phosphate-induced vascular calcification in vitro and in vivo, Kidney Int. 79 (10) (2011) 1071–1079.
[34] S. Elmore, Apoptosis: a review of programmed cell death, Toxicol. Pathol. 35 (4) (2007) 495–516.
[35] P.R. Angelova, A.Y. Abramov, Role of mitochondrial ROS in the brain: from physiology to neurodegeneration, FEBS Lett. 592 (5) (2018) 692–702.
[36] E. Abdelwahid, A. Stulpinas, A. Kalvelyte, Effective agents targeting the mitochondria and apoptosis to protect the heart, Curr. Pharm. Des. 23 (8) (2017) 1153–1166.
[37] R. Anne Stetler, et al., The dynamics of the mitochondrial organelle as a potential therapeutic target, J. Cereb. Blood Flow Metab. 33 (1) (2013) 22–32.
[38] L. Ou, et al., The mechanisms of graphene-based materials-induced programmed cell death: a review of apoptosis, autophagy, and programmed necrosis, Int. J. Nanomedicine 12 (2017) 6633–6646.
[39] Y. Zhang, et al., Autophagy as an emerging target in cardiorenal metabolic disease: from pathophysiology to management, Pharmacol. Ther. 191 (2018) 1–22.
[40] L. Panh, et al., Coronary artery calcification: from crystal to plaque rupture, Arch. Cardiovasc. Dis. 110 (10) (2017) 550–561.
[41] M.J. Budoff, et al., Prognostic value of coronary artery calcium in the PROMISE study (prospective multicenter imaging study for evaluation of chest pain), Circulation 136 (21) (2017) 1993–2005.
[42] M. Helfand, et al., Emerging risk factors for coronary heart disease: a summary of systematic reviews conducted for the U.S. Preventive Services Task Force, Ann. Intern. Med. 151 (7) (2009) 496–507.
[43] J.H. Kim, et al., Lactate dehydrogenase-A is indispensable for vascular smooth muscle cell proliferation and migration, Biochem. Biophys. Res. Commun. 492 (1) (2017) 41–47.
[44] M. Anselmino, et al., Implications of abnormal glucose metabolism in patients with coronary artery disease, Diab. Vasc. Dis. Res. 5 (4) (2008) 285–290.
[45] A. Idelevich, Y. Rais, E. Monsonego-Ornan, Bone Gla protein increases HIF-1alpha-dependent glucose metabolism and induces cartilage and vascular calcification, Arterioscler. Thromb. Vasc. Biol. 31 (9) (2011) e55–e71.
[46] S.J. Lee, et al., Pyruvate dehydrogenase kinase 4 promotes vascular calcification via SMAD1/5/8 phosphorylation, Sci. Rep. 5 (2015) 16577.
[47] J.R. Petrie, T.J. Guzik, R.M. Touyz, Diabetes, hypertension, and cardiovascular disease: clinical insights and vascular mechanisms, Can. J. Cardiol. 34 (5) (2018) 575–584.
[48] Q. Wei, et al., Advanced glycation end products accelerate rat vascular calcification through RAGE/oxidative stress, BMC Cardiovasc. Disord. 13 (2013) 13.
[49] C.Y. Ewald, Redox signaling of NADPH oxidases regulates oxidative stress responses, Immun. Aging Antioxidants (Basel) 7 (10) (2018).
[50] Y. Zhang, et al., Palmitate induces VSMC apoptosis via toll like receptor (TLR)4/ROS/p53 pathway, Atherosclerosis 263 (2017) 74–81.
[51] Y. Chen, et al., Dexmedetomidine Ameliorates Acute Stress-Induced Kidney Injury by Attenuating Oxidative Stress and Apoptosis through Inhibition of the ROS/JNK Signaling Pathway, 2018 (2018), p. 4035310.
[52] B. Chen, et al., N-(3-oxo-acyl) homoserine lactone induced germ cell apoptosis and suppressed the over-activated RAS/MAPK tumorigenesis via mitochondrial-dependent ROS in C. Elegans, Apoptosis 23 (11–12) (Dec 2018) 626–640.
[53] K. Marycz, et al., Evaluation of Oxidative Stress and Mitophagy during Adipogenic Differentiation of Adipose-Derived Stem Cells Isolated from Equine Metabolic Syndrome (EMS) Horses, 2018 (2018), p. 5340756.
[54] D.A. Kubli, A.B. Gustafsson, Mitochondria and mitophagy: the yin and yang of cell death control, Circ. Res. 111 (9) (2012) 1208–1221.
[55] M. Xu, et al., Ghrelin improves vascular autophagy in rats with vascular calcification, Life Sci. 179 (2017) 23–29.
[56] X.Y. Dai, et al., Phosphate-induced autophagy counteracts vascular calcification by reducing matrix vesicle release, Kidney Int. 83 (6) (2013) 1042–1051.
[57] S. Agnihotri, et al., PINK1 is a negative regulator of growth and the Warburg effect in glioblastoma, Cancer Res. 76 (16) (2016) 4708–4719.
[58] S. Rikka, et al., Bnip3 impairs mitochondrial bioenergetics and stimulates mitochondrial turnover, Cell Death Differ. 18 (4) (2011) 721–731.
[59] M.N. Quinsay, et al., Bnip3-mediated mitochondrial autophagy is independent of the mitochondrial permeability transition pore, Autophagy 6 (7) (2010) 855–862.
[60] A. Hamacher-Brady, et al., Response to myocardial ischemia/reperfusion injury involves Bnip3 and autophagy, Cell Death Differ. 14 (1) (2007) 146–157.
[61] K.M. Regula, K. Ens, L.A. Kirshenbaum, Inducible expression of BNIP3 provokes mitochondrial defects and hypoxia-mediated cell death of ventricular myocytes, Circ. Res. 91 (3) (2002) 226–231.
[62] L. Wang, et al., Autophagy induced by low concentrations of crotonaldehyde promotes apoptosis and inhibits necrosis in human bronchial epithelial cells, Ecotoxicol. Environ. Saf. 167 (2018) 169–177.
[63] R. Toita, et al., Protein kinase a (PKA) inhibition reduces human aortic smooth muscle cell calcification stimulated by inflammatory response and inorganic phosphate, Life Sci. 209 (2018) 466–471.
[64] N. Prieto-Dominguez, et al., Melatonin enhances sorafenib actions in human hepatocarcinoma cells by inhibiting mTORC1/p70S6K/HIF-1alpha and hypoxia-mediated mitophagy, Oncotarget 8 (53) (2017) 91402–91414.
[65] X. Wu, et al., Phylogenetic and molecular evolutionary analysis of mitophagy receptors under hypoxic conditions, Front. Physiol. 8 (2017) 539.
[66] S. Langhammer, et al., LDH-A influences hypoxia-inducible factor 1alpha (HIF1 alpha) and is critical for growth of HT29 colon carcinoma cells in vivo, Target. Oncol. 6 (3) (2011) 155–162.